

The EUTELSAT in-orbit test system

K. D. FULLETT, B. J. KASSTAN, W. D. KELLEY, V. E. RIGINOS,
P-H. SHEN, S. L. TELLER, AND Y. THARAUD

(Manuscript received November 3, 1992)

Abstract

An integrated suite of microwave measurement equipment, computer hardware, and measurement software was designed, fabricated, and installed into a unified test facility for measuring the communications subsystem performance of European Telecommunications Satellite Organization (EUTELSAT) communications satellites. The EUTELSAT in-orbit test (IOT) system software supports UNIX-based multiuser, multi-tasking operation in a networked environment that permits remote access and control of the IOT measurement hardware and includes a scheduler that permits unattended stability measurements. The system's human-machine interface offers point-and-click menu selection and input via a mouse device.

The EUTELSAT IOT facility incorporates a dedicated earth station command and control system computer for earth station status checking and configuration, automatic satellite saturation control hardware, and a radiometer for reading atmospheric attenuation. New tests include a method for quickly measuring the frequency response of a spacecraft channel, as well as procedures for measuring AM-to-PM conversion and AM-to-PM transfer coefficient. In addition, the satellite is used as a far-field calibrated signal source for earth station verification and assistance, which enables EUTELSAT to independently test new or existing earth stations for EIRP, gain-to-noise temperature ratio, transmit polarization isolation, and transmit antenna pattern.

Introduction

Following successful launch of a communications satellite, it is desirable to test the communications subsystem in orbit [1]–[3]. Data measured during in-orbit test (IOT) are compared with prelaunch data to determine whether the

subsystem has successfully survived launch and meets performance specifications. The technical objective of IOT is to measure the communications performance of the satellite under test as completely and accurately as possible. IOT is performed for acceptance testing immediately after launch; to monitor communications subsystem performance throughout the satellite's operational lifetime; and to investigate anomalies [4]. It may also be performed prior to the satellite being sold, or in preparation for carrying new services. These missions determine the basic requirements of the IOT system.

In a laboratory environment, a device under test is near at hand; however, a geostationary satellite is located about 42,000 km from the earth station and the IOT equipment [1],[3], which significantly complicates testing and measurement. For example, one-way signal attenuation from 180 to 215 dB is encountered at the test frequencies, and atmospheric variability along the propagation path must be accounted for. To obtain the desired accuracy and repeatability, precise calibration of the test setup, earth station equipment, and antennas is of paramount importance. On the other hand, the geometry and location of the satellite are ideal for accurately measuring the satellite's far-field antenna patterns, since prelaunch antenna patterns are generally measured on non-ideal ranges. In addition, the satellite serves as a far-field calibrated signal source for earth station verification measurements [5]. By moving the earth station antenna in a predetermined manner while measuring the strength of a test carrier received from the satellite, the pattern of the earth station receive antenna can be accurately measured.

Newer satellites provide more transponders and have greater payload complexity than earlier generations [1],[3],[6]. This trend places increased demands and constraints on the IOT systems built to test them. Because owners desire to place their satellites into revenue-generating operation as soon as possible after launch, the IOT system is expected to perform as quickly as possible, especially during acceptance testing, and to use a minimum of on-board fuel in order to maximize the useful lifetime of the spacecraft [1],[3]. Due to the increased satellite capacity and complexity, the testing process generates large volumes of data that must be maintained and reported. Finally, the pool of spacecraft experts available for performing complex IOTs and evaluating the resulting data is distributed more thinly as the number of satellite networks in service [6] increases.

Although in-orbit measurement is its primary technical objective, the IOT system must also address other requirements such as real-time operation, human/computer interaction, networking, and remote access and control of the measurement hardware. The system must provide a user interface that is easy to use, yet flexible enough to accommodate the various IOT missions. The

capability to execute measurements concurrently and to support a multiuser environment are desirable system features.

IOT technology and techniques have advanced in parallel with communications satellite technology, facilitated by the availability of more powerful, less costly computing hardware and software, as well as newer "smart" instruments that contain their own processors. Major advances were made in IOT from one satellite series to the next for the INTELSAT III, IV, IV-A, and V satellites, and many of the fundamental IOT measurements performed 20 years ago are still in use today [1]–[4]. The development of the modern, computer-controlled IOT system is traced in References 1, 3, and 6.

IOT measurements are performed by transmitting test signals to the spacecraft and comparing their power, frequency, and phase with the signals retransmitted from the satellite. Fundamental measurements include spacecraft input power flux density (IPFD) and equivalent isotropically radiated power (EIRP), transponder in-band and out-of-band frequency response, gain transfer, group delay, and gain-to-noise temperature ratio, G/T . Over the years, many other measurements have been developed as well [1]–[5].

This paper discusses some of the innovative system features and new IOT measurements implemented in the European Telecommunications Satellite Organization (EUTELSAT) IOT system. For example, the EUTELSAT IOT facility interacts directly with the earth station command and control system (ECCS) computer, incorporates radiometric information, and uses an automatic satellite saturation controller (ASSC) in the earth station. The facility also implements new techniques for rapidly measuring the in-band frequency response of a communications satellite's transponders and for verifying the performance of a second earth station, using the spacecraft as a far-field calibrated signal source. The system's software also incorporates many new features, such as the ability to perform unattended measurements automatically at any scheduled time. The system software runs under the multiuser, multitasking UNIX operating system in a networked environment that permits remote control and access of the IOT measurement equipment and enables it to execute in a multicomputer, distributed processing network.

The user interacts with the IOT system via an X-Window-based graphical display, using a mouse to select items from a menu. Measurements are specified in a "form-fill-in" format, rather than the traditional "remember-and-type" command line interface found on many systems. The effectiveness of such graphically based user interfaces is supported by more than 30 years of research and development (e.g., Reference 7).

IOT system requirements and constraints require that more of the system functionality reside in the software, which must initially address the network,

hardware, and communications environment of a distributed processing system capable of supporting a number of workstations. With development and continuous refinement over the last decade, the Measurement Processing and Control Platform (MPCP) has served as the software foundation for the EUTELSAT IOT system described here. The principal software concepts and innovations underlying implementation of the MPCP are discussed in a companion paper [8].

IOT hardware

The EUTELSAT IOT system consists of a suite of microwave measurement equipment, computer hardware, and measurement software integrated into a unified test facility for measuring the communications subsystem performance of EUTELSAT satellites. The design and operation of this IOT system are discussed in References 4 and 5, and other system features are described in Reference 6. The IOT facility, installed at the Rambouillet earth station near Paris, France, has been used to test the EUTELSAT II spacecraft, F1 through F4.

The major components of the EUTELSAT IOT facility, depicted in Figure 1, are the IOT equipment (IOTE), the earth station equipment, and the dual-polarization transmit/receive antenna. A station radiometer connects to a second antenna. The IOTE comprises microwave measurement system (MMS) hardware and the IOT workstation and peripherals.

The earth station equipment receives uplink signals generated by the IOT hardware, amplifies them, and transmits them to the antenna system. It then receives downlink signals from the spacecraft, amplifies them, and transmits them to the IOTE for measurement. The IOTE supports dual-polarization measurements and accommodates the 14- to 14.5-GHz uplink band and the three downlink bands that fall in the 10.95- to 12.75-GHz frequency range of the EUTELSAT II satellites.

In earlier IOT systems, earth station information was obtained directly from a station operator. The EUTELSAT IOTE interacts with the ECCS computer to monitor and control the earth station equipment. The IOT workstation sends commands via an interconnecting IEEE-488 bus cable to the ECCS computer. For example, the IOT workstation may request uplink power meter readings or the power level and frequency settings on the inject synthesizer. The computer performs the requested operations and returns responses to the IOT workstation.

The ECCS computer, supplied by Direction des Reseaux Exterieurs de FRANCE TELECOM (DTRE), can perform the following measurement-related functions:

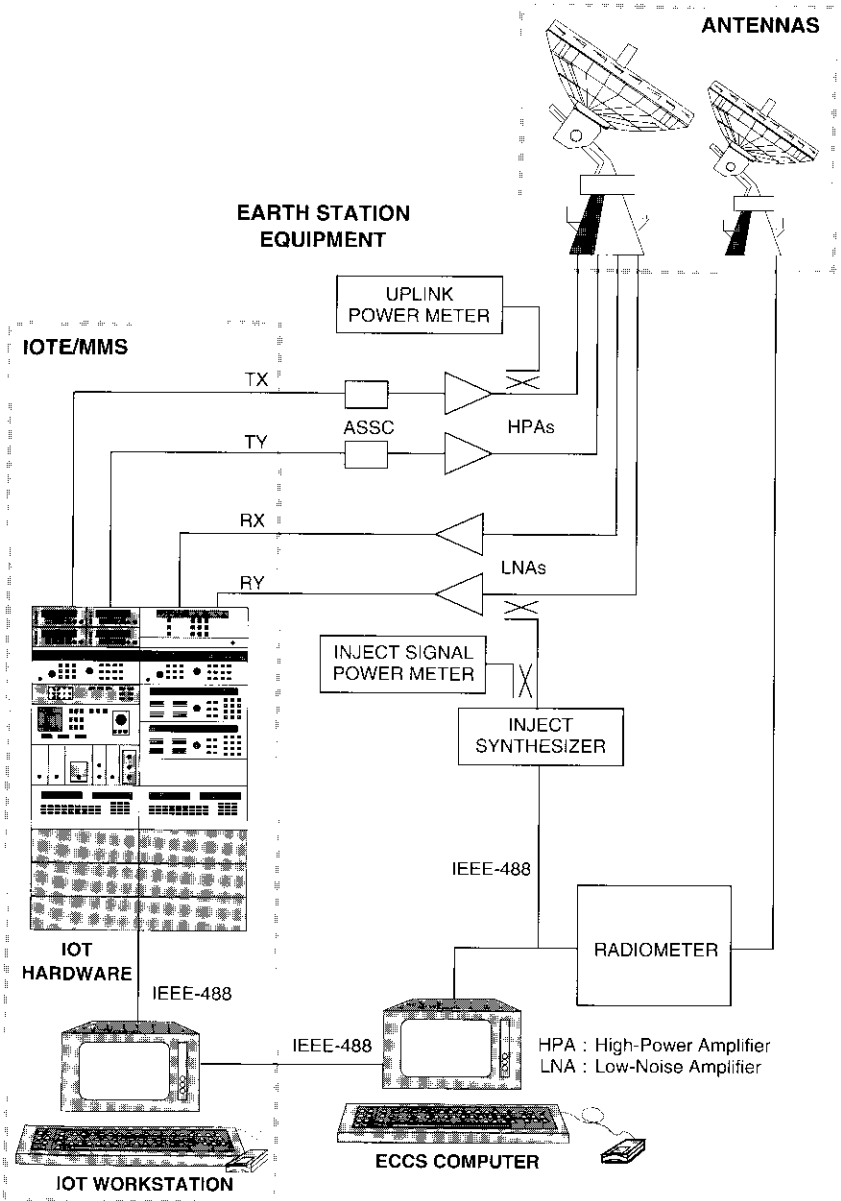


Figure 1. EUTELSAT IOT System Block Diagram

- Control the injected signal power and frequency as commanded by the IOT workstation.
- Control the uplink power level and perform power-leveling as the frequency is varied.
- Control the ASSC equipment to determine the saturation power level.
- Provide a radiometer reading to the IOT workstation on command.
- Read the uplink power meter at the feed and provide the calibrated readings to the IOT workstation.
- Provide the antenna gain and coupler calibration values for any operational uplink or downlink frequency.
- Provide the azimuth and elevation antenna position to the IOT workstation.
- Configure the earth station on command from the IOT workstation.
- Zero and calibrate the uplink and inject signal power meters.

IOT systems must be capable of determining the saturation flux density of the spacecraft. One method that has been used successfully is the amplitude-modulated (AM) nulling technique, described in the IOT system literature (*e.g.*, References 1 and 2). In early IOT systems, AM nulling was applied manually; the EUTELSAT IOT uses the ASSC to perform this function automatically. The ASSC maintains the satellite at saturation, and was designed to meet EUTELSAT specifications [4]. It operates over a large dynamic range of satellite gain.

The ASSC automates the AM nulling technique to determine saturation flux density, as follows. First, an AM carrier is transmitted to the spacecraft. On the downlink, after envelope detection, the AM carrier is phase-locked to the AM source, producing an error voltage proportional to the modulation amplitude, which decreases as saturation is approached. The error voltage is interpreted by the digital processor, which commands the uplink earth station EIRP. As saturation approaches, the EIRP is controlled in 0.05-dB steps. When the error voltage reaches a minimum, saturation has been achieved. Since the ASSC operates as a closed loop, any variation in uplink propagation conditions is counteracted by the detected error voltage, the sign of which governs the relative polarity of the uplink EIRP.

The IOT setup must take into account not only instrumentation, earth station equipment, and antenna uncertainties, but also the RF path between the station and the spacecraft [1],[3]. In the EUTELSAT IOT system, the measurement program obtains atmospheric attenuation data from a radiometer. The radiometric configuration consists of a Cassegrain antenna connected to a noise-injection-type radiometric receiver, and a computer to control operation, pro-

cess the measurement data and perform housekeeping functions [4]. Attenuation calculated at 13 GHz is scaled to other frequencies by the radiometer's computer, using standard frequency-scaling equations. Over the short time period typical of an IOT measurement (a few minutes), the change in atmospheric attenuation is assumed to be negligible.

Figure 2 is a simplified block diagram of the EUTELSAT IOTE MMS hardware configuration. A high-stability, 10-MHz reference signal output by uplink synthesizer 1 (UL Syn 1) is amplified and distributed to the IOT instruments as a common reference signal. The IOT workstation communicates with the instruments via three IEEE-488 buses, and with the ECCS computer via a fourth IEEE-488 bus.

Two test carriers are provided by two RF synthesizers. UL Syn 1 outputs an RF test carrier, as commanded by the IOT workstation. The synthesizer's RF output can be frequency-modulated by an externally supplied modulation signal to disperse the uplink energy, in order to meet the downlink earth surface spectral density specifications of the International Radio Consultative Committee (CCIR) 358-2 during routine operation. Because the synthesizer does not operate over the required uplink frequency range, a 12-times frequency multiplier is employed.

Uplink synthesizer 2 (UL Syn 2) is capable of generating an RF output test signal anywhere in the uplink frequency range. The synthesizer's RF output (in the 14- to 14.5-GHz range) can be amplitude-modulated externally (via the modulator shown in Figure 2) when necessary—for example, when group delay is measured.

An uplink switching/coupling matrix provides flexible uplink configurations and is necessary to support all IOT measurements. The RF output from either synthesizer can be switched and routed to either transmit polarization waveguide, TX or TY. When required, the IOTE can produce two carriers on one of the two polarizations, or a single carrier on each polarization, to support two-tone measurements such as third-order intermodulation, CI_3 .

As shown in Figure 2, the spectrum analyzer (SA) can be switched, via the 8-pole switch, to input the uplink polarization (TX or TY), the received signal (RX or RY, selected by another switch), the IF synthesizer output, or the output from the phase measurement subsystem. Additionally, the spectrum analyzer can be switched to input a sample of either high-power amplifier (HPA) output signal, as well as to receive an input signal from a front panel connector. The video output of the spectrum analyzer can be switched to provide an input to either the network analyzer or the digital voltmeter. The analyzer's IF output can be switched to provide an input to either the modulation analyzer or the frequency counter. The switch configurations for all

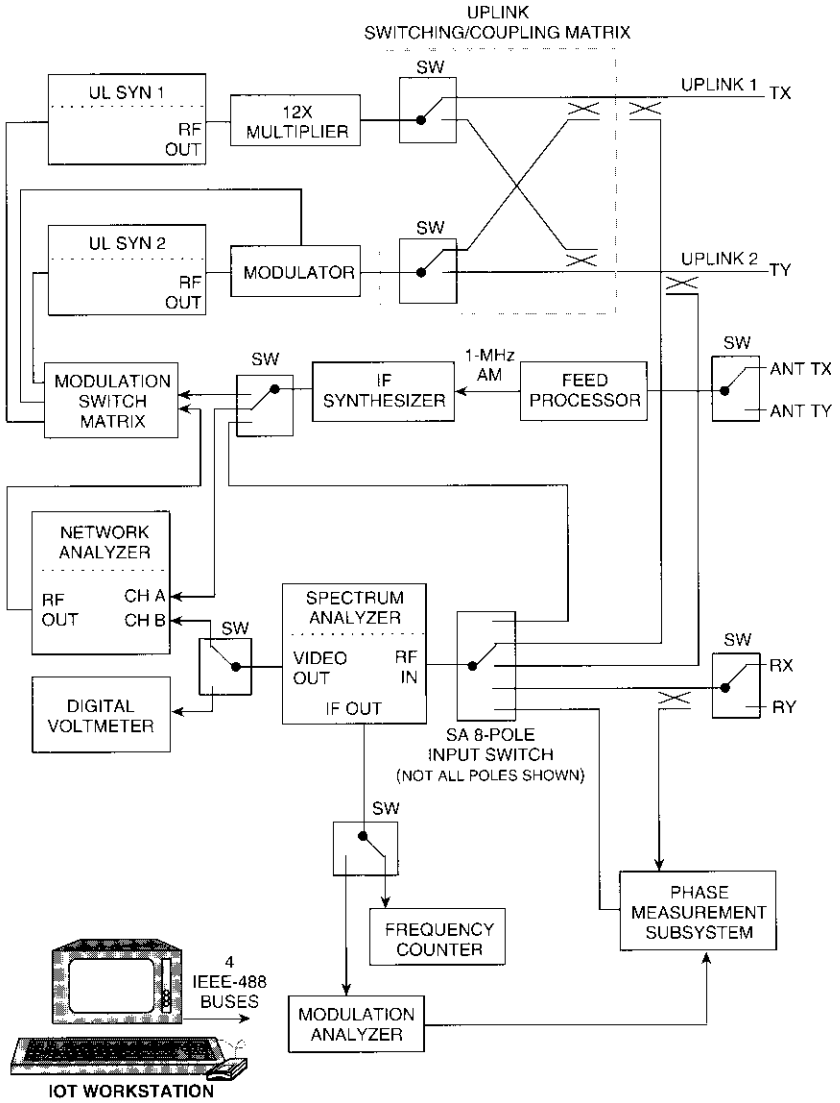


Figure 2. IOTE Microwave Measurement System Block Diagram

measurements are controlled by the IOT workstation via RF switch controllers and IEEE-488 buses.

The feed processor, which is used for measurements such as group delay, performs the following function. When the uplink carrier produced by UL Syn 1 or UL Syn 2 is amplitude-modulated, the modulation is detected by diode detectors located near the antenna feed. Typically, the AM frequency is around 1 MHz. The detected modulation is transmitted to the input of the feed processor, which can be switched to select either of the uplink polarizations (ANT TX or ANT TY in Figure 2). The feed processor amplifies and filters the detected modulation, and supplies it to the IF synthesizer as a reference. The synthesizer's 1-MHz, frequency-adjusted output is fed into the network analyzer, which measures its phase relationship with respect to the Doppler-shifted 1-MHz modulation on the carrier received by the spacecraft.

The phase measurement subsystem is used to perform phase noise measurements on the received RF signal, such as ΔM -PM conversion, AM-PM transfer coefficient, and spurious modulation. It consists of a down-converter, a phase reference synthesizer, and a dedicated low-frequency spectrum analyzer.

An important innovation of the EUTELSAT IOT system is its ability to perform unattended stability measurements. While measurements are normally performed with operator interaction, some can be executed in a non-interactive mode if directed by the user via the X Window interface. The EUTELSAT IOT system allows the user to specify measurements to execute at any scheduled time and at specified intervals throughout a specified duration.

The ability to schedule measurements and to have them execute periodically provides the basis for performing stability measurements, which track various quantities as a function of time. For example, the EIRP measurement can be scheduled to run every hour over a 24-hr period to determine EIRP variation. Stability measurements can be performed for spacecraft EIRP, spacecraft IPFD, in-band and out-of-band transponder frequency response, spacecraft G/T , beacon EIRP, and beacon frequency.

The IOT system scheduler launches measurements at the scheduled time and allocates resources to a measurement that has requested them. It also manages scheduling conflicts between two or more measurements on a first-come, first-served basis. When a measurement completes execution, it returns resources such as the spectrum analyzer and other measurement instruments to the scheduler, which makes them available to the next scheduled measurement. The operation of the IOT scheduler, and its interaction with the measurement user interface program and the actual measurement program (which are

separate programs that can execute on different workstations and at different times), are described in the companion paper [8].

The IOTE is controlled by a 32-bit, reduced instruction set computing (RISC)-based engineering workstation with 16 Mbytes of memory and a 600-Mbyte hard disk for program and data storage. The workstation executes IOT system and measurement software to perform IOT measurements and to process, store, and retrieve measurement data. The software runs under a licensed version of the UNIX System V operating system. The IOT workstation controls the microwave measurement hardware and communicates with the ECCS computer across an IEEE-488 bus. It also communicates with the user via an X-Window-based, graphical user interface with keyboard and mouse input. The workstation supports connection to an IEEE 802.3 local area network (LAN). Its peripherals include a 19-in., high-resolution, color bit-mapped display; a multipen plotter; a printer; a cathode-ray tube (CRT) terminal; and a 9,600-bit/s modem for remote access and control. The IOT software is described in detail in Reference 8.

Standard IOT measurements

Most satellite communications payload parameters, such as antenna patterns, EIRP, and receive G/T , can be derived from fundamental measurements of microwave power and frequency [3]. During the past 20 years, the evolution of IOT measurement techniques has been governed by the increasing complexity of communications payloads and the requirement to place the spacecraft into operational service as quickly as possible while minimizing consumption of onboard fuel. Continuous refinement of measurement techniques has permitted more parameters to be measured with a higher level of confidence. This has resulted in an expanding amount of data from the increased number of transponders and connectivity configurations [1],[3].

For each IOT measurement, all uncertainties must be identified and accounted for in an error budget. The total root-sum-square (RSS) uncertainty resulting from all error sources is computed for each measurement. As discussed in Reference 9, uncertainties can arise from the spacecraft (antenna pointing, platform stability, and repeatability of switching), atmospheric loss and variability, the earth station (antenna calibration and pointing, up and downlink coupler calibration), and measurement instrumentation. Numerical uncertainties due to digital processing of raw measurement data within the workstation must be considered for some measurements, such as the "Fastswep" measurement described later.

The human operator is another potential source of measurement error (*e.g.*, improper use of instrumentation, lack of skill, and improper measurement

technique). Human interface engineering can detect and prevent (or minimize) operator errors, as discussed in References 6 and 8.

To enhance measurement accuracy, the measurements of absolute quantities necessary for an IOT have been reduced to microwave power, frequency, and phase [1]; all other measurements are relative to, or can be derived from, these values. For the uplink, transmit power is measured directly by a directional coupler that provides power from the uplink waveguide to a power meter.

The EUTELSAT IOT system performs a large number of measurements that can be grouped according to the basic quantity measured: power, frequency, or phase.

Power measurements

The fundamental power measurement performed by an IOT system is the accurate measurement of spacecraft EIRP. Many other measurements are derived from the EIRP, including the point-to-point transponder frequency response and gain transfer measurements.

For measuring downlink signals, an injected carrier technique has proved to be the best approach and continues to be used in IOT systems [1]–[3]. A locally generated carrier (the inject signal) is offset slightly in frequency from the carrier received from the satellite, and is injected via a directional coupler into the waveguide between the receive antenna feed and the low-noise amplifier (LNA), as shown in Figure 1. After amplification by the LNA (and additional amplifiers, if necessary), both the received and injected signals are displayed on the spectrum analyzer and measured. The difference is used by the EIRP program to adaptively adjust the injected signal power to within about 1 dB of the received signal. The final difference is then measured by the spectrum analyzer, and the power level of the final injected carrier is measured precisely by a power meter. Based on this knowledge of the injected signal level and its difference from the received signal level, the level of the received signal (even if noisy) can be determined to within a few tenths of a decibel. This adaptive technique ensures a wider dynamic range, while reducing logarithmic amplifier errors within the spectrum analyzer. The injected carrier technique permits accurate measurement of received continuous-wave (CW) carriers and is unaffected by any change in the gain of the receive chain. The calibration effort can thus be restricted to a few passive microwave components, such as the inject coupler [1].

The spacecraft EIRP is computed from the measured injected signal power meter reading, the level difference measured by the spectrum analyzer, the inject signal coupler value, the downlink antenna gain at the frequency of

interest, the downlink path loss, and the downlink atmospheric loss. Spacecraft EIRP measurement using the injected signal technique is well established and has been described in earlier IOT literature (*e.g.*, References 1 and 2.)

The EUTELSAT IOT system performs the following power measurements and monitoring functions:

- EIRP (downlink only, with no uplink test signal from the IOT station)
- Combined spacecraft IPFD and spacecraft EIRP
- Amplitude linearity (gain transfer) and intermodulation (CI_3)
- G/T and G/T stability
- Point-to-point frequency response (in-band, in-band stability, out-of-band, and out-of-band stability)
- Fastsweep frequency response
- Overall cross-polarization isolation
- Receive and transmit cross-polarization
- Antenna pattern
- Gain adjustment
- Spurious output
- Beacon measurements (EIRP, EIRP stability, cross-polarization isolation)
- Communications system monitoring (CSM)
- Payload monitoring (IPFD/EIRP, linear gain, gain transfer, local oscillator frequency)
- Earth station verification and assistance (ESVA).

The Fastsweep and ESVA measurements are new with the EUTELSAT IOT system, and are described later in this paper.

Frequency measurements

Frequency measurements are the second category of fundamental measurements performed by an IOT system. The EUTELSAT IOT system can measure frequency conversion error and stability, beacon frequency and beacon frequency stability, and routine spacecraft payload monitoring (RSPM) frequency conversion error. Since the uplink frequency and nominal spacecraft local oscillator frequency are known, the spectrum analyzer (Figure 2) can be tuned to the nominal downlink frequency, where it performs peak and zero-span measurements. The frequency of the analyzer's IF output is measured precisely by the counter. The measured received signal frequency offset from the

center frequency of the analyzer IF is used in conjunction with the analyzer's tuned microwave frequency to fine-tune the analyzer to the frequency of the received signal. This technique is employed in all IOTE measurements to ensure that the spectrum analyzer is tuned precisely to the received signal frequency, so that power measurements are performed accurately.

For some measurements in which the precise frequency is the objective, the IOTE can correct for the Doppler shift caused by non-zero radial velocity between the spacecraft and the earth station. For example, in measuring the spacecraft local oscillator frequency, the IOT user interface permits the user to specify that Doppler correction be performed. The measurement then computes the Doppler-effect frequency contribution, based on the velocity, and corrects the received frequency.

Phase noise measurements

The EUTELSAT IOT phase measurement subsystem, shown in Figure 2, measures the AM-PM conversion coefficient, K_p ; AM-PM transfer coefficient, K_t ; and spurious modulation. The AM-PM conversion and transfer coefficient measurements are new, and are described in the next section.

New measurements

Among the system features mentioned above are several new measurements implemented in the EUTELSAT IOT system: Fast sweep frequency response, AM-PM conversion coefficient, AM-PM transfer coefficient, and several ESVA measurements (EIRP, G/T , transmit polarization isolation, and transmit antenna pattern).

Fast sweep frequency response measurement

Measurement of a spacecraft channel's frequency response is a fundamental IOT system requirement. The standard technique measures the response point-to-point throughout the band of interest. Because of the larger number of channels on board the latest generation of communications satellites, such as EUTELSAT II, measuring the frequency response of all channels requires substantial testing time. Since this activity deprives the satellite owner of revenue, there is continual pressure on IOT systems designers to shorten the time required for IOT.

A new technique called Fast sweep has been developed which measures frequency response by continuously sweeping the desired spacecraft channel, while simultaneously measuring the received downlink signal on the spectrum

analyzer. The synthesizer generating the swept uplink signal sweeps much slower than—and is not synchronized to—the spectrum analyzer measuring the received downlink signal. Raw measurement data are captured digitally by the spectrum analyzer and read into the computer for numerical post-processing and to determine the frequency response. Because most of the measurement processing is performed in the computer, standard equipment such as the HP-8673E synthesizer and HP-8566B spectrum analyzer can be used to obtain the raw data. No special equipment is required to synchronize the sweeps of the two instruments.

It is instructive to examine the traditional IOT point-to-point measurement technique in terms of the time it requires. The technique consists of a combination of EIRP and IPFD measurements repeated over a set of predetermined discrete frequencies across the bandwidth of interest. The frequency response of a transponder is determined by measuring downlink power relative to a band-center measurement in either the linear or saturated region of the traveling wave tube amplifier (TWTA) frequency band of the transponder under test, with the uplink power kept constant as the frequency is varied. Measurement at saturation gives the frequency response of all filters after the output TWTA, while measurement in the linear region gives the overall frequency response.

Initially, the system is tuned to the channel center frequency and the IPFD is measured at saturation, as described in References 1 and 2. The uplink power is then reduced to an operator-specified backoff level, and the system is tuned to the lowest frequency to be measured. The IPFD is measured at each frequency and used in conjunction with the EIRP measurement to calculate the transponder gain, thus compensating for uplink power variations due to changes in uplink frequency. The frequency is then stepped to the next discrete frequency, and the gain is again calculated. This process is repeated until the transponder gain has been measured at all frequencies in the desired band. Measurements of EIRP and IPFD employ radiometric data to account for atmospheric attenuation.

The point-to-point frequency response measurement uses the injected signal technique, described earlier and in References 1 and 2. A limitation of this approach is the measurement time required. For each frequency point, the uplink synthesizer is tuned and the spectrum analyzer waits approximately 240 ms for the downlink signal. The analyzer is tuned to the received signal and measures it. The inject synthesizer is then tuned by the FCCS computer. The spectrum analyzer is retuned to the inject signal and measures it. At least one adjustment of the inject synthesizer power level is necessary to bring the received and injected signal levels to within 1 dB of each other. Each adjust-

ment is commanded through the ECCS. Finally, the inject power meter is read. These operations typically require a few seconds per frequency point, with the majority of time being associated with ECCS communications and reading the power meter. Thus, measuring a 40-MHz channel in 1-MHz steps requires about 8 minutes.

By comparison, Fastswep measures the frequency response of a spacecraft channel in a much shorter time, but with some reduction in accuracy and dynamic range. The accuracy of Fastswep, with earth station correction, is 0.27-dB RSS uncertainty, as compared with 0.17-dB RSS uncertainty for point-to-point measurement performed in the linear region of the TWTA.

Typically, Fastswep measures the response of a 40-MHz channel in approximately 8 s, and an 80-MHz channel in approximately 10 s, plus a display time of about 1 s. The dynamic range of the measurement is approximately 50 dB, exclusive of limitations within the earth station. By comparison, the stepped point-to-point measurement has a dynamic range in excess of 80 dB; however, the measurement time is considerably longer. The Fastswep measurement configuration is depicted in Figure 3.

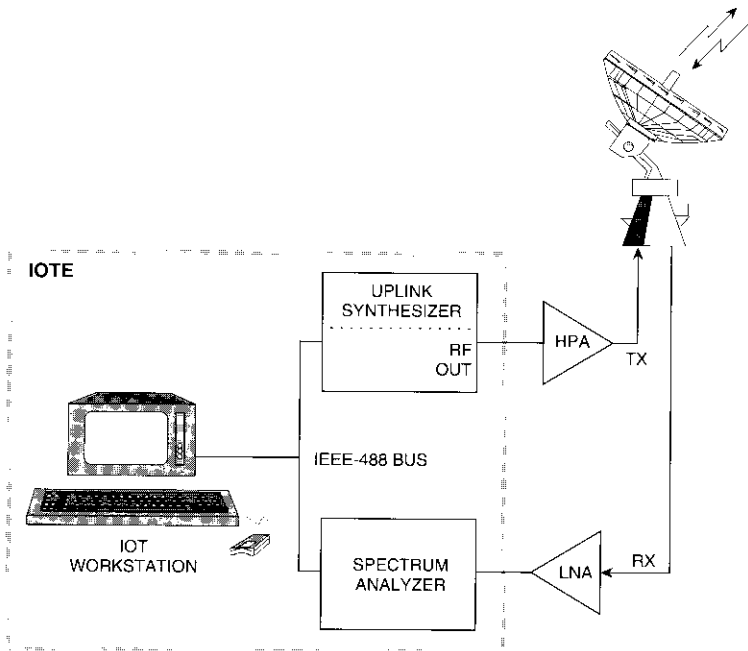


Figure 3. *Fastswep Measurement Configuration*

Fastsweep generates a frequency response that is relative in both frequency and power to band center. The major factors contributing to uncertainty in the Fastsweep method within the filter passband are the gain slope in the uplink, the ability to rapidly level the uplink power over the measurement bandwidth, the downlink gain slope, and the spectrum analyzer gain slope over any 80-MHz bandwidth.

If requested by the operator during measurement specification, the earth station noise contribution can be taken into account by pointing the earth station antenna to the sky and performing a Fastsweep when no downlink signal is present. Several Fastsweep calibration measurements may be performed and averaged to lessen the effect of noise variation. The resultant noise-only Fastsweep, which includes the nonlinearities of the earth station receive chain, is stored in an earth station calibration file and can be used to correct the Fastsweep measurements of spacecraft transponders. Calibration measurements are performed for each receive polarization across each of the three EUTELSAT II downlink receive bands.

Fastsweep is performed in two phases: sweeping of the uplink by the uplink synthesizer, and measurement of the received downlink by the spectrum analyzer. This is followed by numerical post-processing to extract the frequency response from the raw data. When the measurement phase begins, the synthesizer generates a frequency sweep over the desired uplink band, the amplitude of which is leveled by the leveling loop controlled by the ECCS computer. For each sweep, the synthesizer outputs a sequence of discrete, rather than continuous, frequencies. The synthesizer dwells at each frequency for the minimum time that allows several measurements (*i.e.*, spectrum analyzer sweeps) of the received signal by the spectrum analyzer, as illustrated in Figure 4.

While the synthesizer is sweeping the uplink, the spectrum analyzer continuously sweeps the received signal, asynchronously with respect to the synthesizer sweeps, using the max-hold measurement mode. The resolution bandwidth is chosen to optimize sweep speed *vs* the measurement signal-to-noise ratio, S/N . Smaller bandwidths require a much longer sweep time, while larger bandwidths degrade the available carrier-to-noise power density ratio, C/N_0 . Typically, a 100-kHz-resolution bandwidth is used.

After a sufficient number of analyzer sweeps, the measurement phase terminates and the data processing phase commences. The measurement program reads the stored trace from the spectrum analyzer, which contains N frequency-*vs*-amplitude data points (f_i, A_i) , where $i = 1, \dots, N$. For the HP-8566B spectrum analyzer used in the EUTELSAT IOTE, $N = 1,001$. The amplitude value, A_i , for each data point is the peak power that was measured at

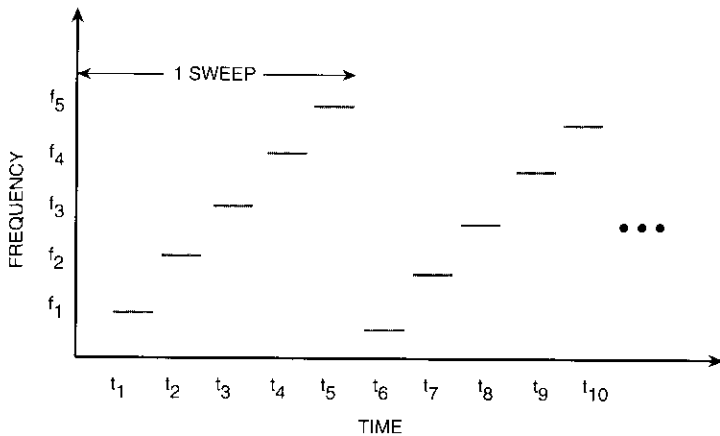


Figure 4. *Synthesizer Output vs Time*

frequency f_i during the entire measurement phase. The array of measured data points read from the analyzer is time-sequenced, such that the i th frequency, f_i , always occurs earlier than the $(i + 1)$ frequency, f_{i+1} . The trace read from the spectrum analyzer resembles the one shown in Figure 5.

As can be seen in the figure, the trace contains peaks and valleys. Peaks are actual measurements of the downlink signal, while valleys are signal dropouts that occur during the frequency step transitions of the synthesizer and the retraces of the synthesizer sweep. The dropouts are signal fades, which are measurement artifacts that occur because the spectrum analyzer and synthesizer sweeps are not synchronized. The spectrum analyzer measures noise peaks, rather than the actual signal, during synthesizer switching transitions to new frequencies.

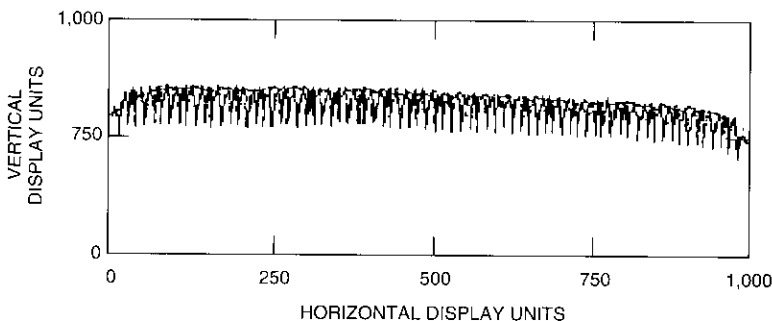


Figure 5. *Fast-sweep Spectrum Analyzer Trace Output*

The desired response can be obtained by extracting the envelope of the trace data. This is accomplished by numerically post-processing the data, as follows. The analyzer trace depicted in Figure 5 can be viewed as a time-sequenced "signal" with low-frequency components (*i.e.*, the envelope that is the desired response) and high-frequency components (the signal dropouts). The envelope can then be extracted by applying a numerical low-pass filter to the "signal." The filter consists of a fast Fourier transform (FFT) operation on the data set, followed by removal of high-frequency points, followed by a second FFT. A peak detection is then performed on the filtered data to obtain the envelope.

Although the numerically implemented low-pass filter algorithm removes the systematic high-frequency perturbations contained in the measured data set, random noise in the correlated samples is not removed. To minimize the noise, multiple Fastsweps are performed and averaged. Figure 6 is a typical plot output of a Fastswep.

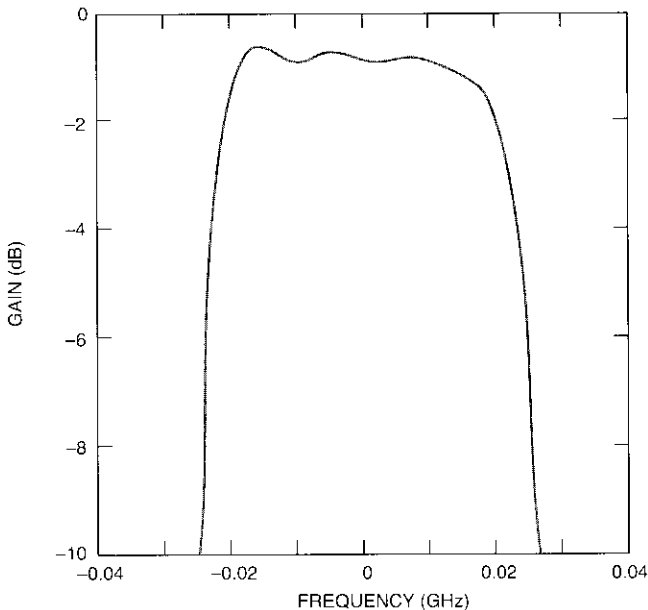


Figure 6. *Fastswep Measurement Plot Output*

AM-PM conversion and phase shift

The AM-PM conversion measurement determines that the AM-PM conversion coefficient, K_p , for each transponder is within the limits specified for drive levels to the TWTA, from 20-dB input backoff to saturation. The total phase shift is calculated by integrating the conversion coefficient phase for comparison with the satellite specification.

In this measurement, the IOTE transmits an amplitude-modulated carrier with a low modulation index at an uplink power level corresponding to 20-dB input backoff of the TWTA. The power level is then stepped up to TWTA saturation in 1-dB steps. For each uplink power level, the corresponding downlink signal is phase-demodulated by the modulation analyzer and the phase measurement subsystem. Using a test translator, the above sequence can be repeated for the earth station loop in order to measure the phase modulation of the earth station receive chain for inclusion in the AM-PM conversion coefficient computation. The coefficient, K_p , is then plotted against the TWTA input backoff.

The measurement sequence proceeds as follows. First, a calibration procedure (described below) is performed and the synthesizer is amplitude-modulated via the external PIN modulator (see Figures 2 and 7 for the hardware configuration). The power level of the modulated carrier is then adjusted to the user-specified backoff level. The demodulated tone, output by the modulation analyzer (HP-8901A), is measured using the low-frequency spectrum analyzer (SA), and data are gathered to perform the K_p computations.

The AM-PM conversion measurement employs the phase measurement subsystem of Figure 2, which consists of an HP-11729C carrier noise test set, a low-frequency HP-3582A spectrum analyzer, and an HP-8662B RF synthesizer [10]. The subsystem configuration is depicted in Figure 7.

The instrumentation used to perform the measurement depends on the modulation frequency of the carrier, as shown in the figure. If the modulation frequency is less than or equal to 20 kHz, the modulation analyzer and low-frequency spectrum analyzer are used. If the modulation frequency is greater than 20 kHz, the HP-11729C carrier noise test set may be used.

The K_p calibration procedure is performed as follows. A single CW test carrier is transmitted to the spacecraft to verify test signal levels and the spacecraft local oscillator frequency. The IF synthesizer outputs a calibration signal into the FM port of the uplink synthesizer via the modulation input matrix switch. The modulation voltage is selected to generate a low-deviation FM signal having a nominal phase modulation of 5° peak-to-peak, which

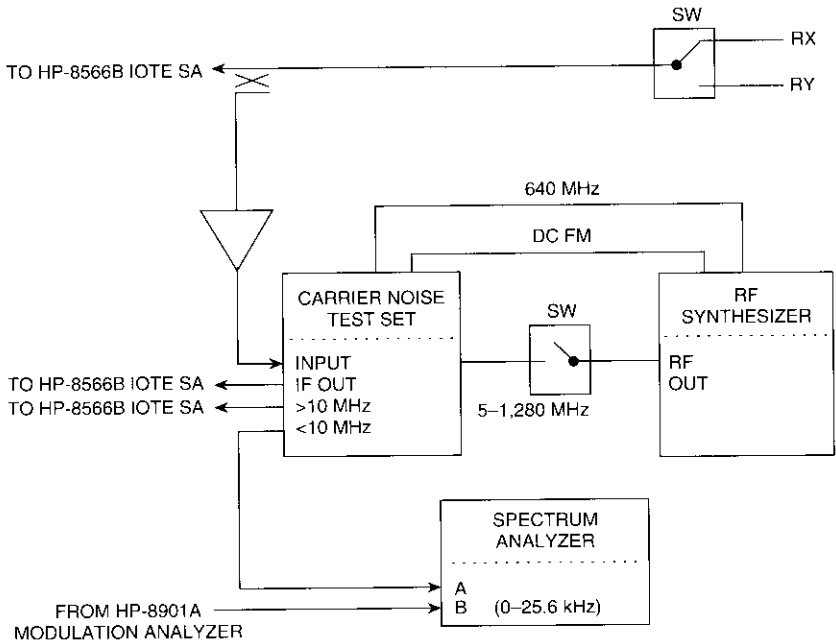


Figure 7. Phase Measurement Subsystem

serves to calibrate the receive chain phase measurement. The spectrum analyzer is then switched to the test uplink path to verify the modulation index. The carrier-to-sideband ratio is measured, adjusted if necessary, and stored. Next, the measurement system, consisting of the spectrum analyzer, modulation analyzer, and low-frequency spectrum analyzer, is connected to the uplink signal. The level of the demodulated tone at the modulation frequency is measured to establish a reference level for the phase deviation (which is about 5° peak-to-peak) and used as a calibration. The uplink signal and FM calibration modulation are turned off, completing the calibration procedure.

The calibration power level (in dBm) measured during the calibration sequence is converted to a voltage, as is the power measured at the baseband spectrum analyzer for each measurement point. The phase is then computed and used as a basis for calculating K_p from the following formulas:

$$V_c = 10^{P_c/20} \quad (\text{V}) \quad (1)$$

$$V_m = 10^{P_m/20} \quad (\text{V}) \quad (2)$$

$$\varphi = \beta \left(\frac{V_m}{V_c} \right) \quad (\text{rad}) \quad (3)$$

$$K_p = \frac{\varphi}{M} \quad (\text{deg/dB}) \quad (4)$$

where

- V_c = equivalent voltage of calibration power (V)
- P_c = measured calibration power (dBm)
- V_m = equivalent voltage of measured power (V)
- P_m = measured phase modulation power level (dBm)
- φ = computed peak-to-peak phase (deg)
- β = peak-to-peak phase during FM calibration (deg)
- K_p = AM-PM conversion coefficient (deg/dB)
- M = measured AM modulation (dB).

Figure 8 shows a typical plot output of a K_p measurement.

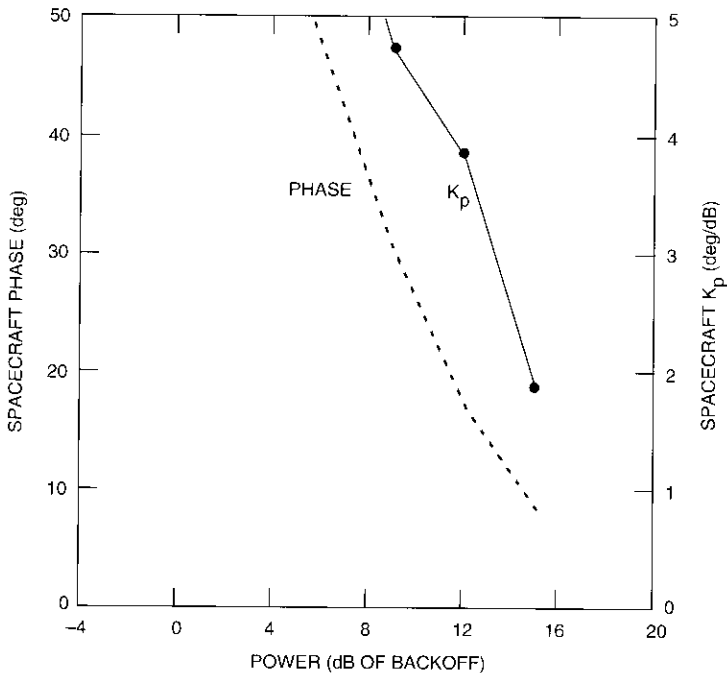


Figure 8. AM-PM Conversion Coefficient Plot Output

AM-PM transfer coefficient

The AM-PM transfer coefficient, K_t , measurement determines the amount of phase modulation imposed on an unmodulated carrier (called the "target") by an amplitude-modulated carrier (called the "source"), which is offset in frequency from the target. The IOT earth station transmits the source and target carriers simultaneously via the two independent uplink chains. After reception of the resulting downlink signal at the IOT station, both carriers are down-converted, and the target signal is passed to the modulation analyzer and phase measurement subsystem to measure its phase modulation. The AM-PM transfer coefficient, K_t , is then computed based on the ratio of the measured phase modulation of the target to the depth of the source AM.

The instrumentation used to perform the measurement depends on the modulation frequency of the source carrier, as shown in Figure 7. If the modulation frequency is less than or equal to 20 kHz, the modulation analyzer and low-frequency spectrum analyzer are used. If the modulation frequency is greater than 20 kHz, the noise test set may be employed.

For the K_t measurement, the phase demodulator is initially calibrated with a 5° peak-to-peak phase-demodulated carrier, exactly as for the K_p measurement. The source carrier from the synthesizer is then amplitude-modulated via the external PIN modulator. The power levels of the modulated source and unmodulated target carriers are adjusted so that the sum of the two is equal to the operator-specified backoff level, and then transmitted to the spacecraft. The demodulated tone output by the modulation analyzer is measured, and data are gathered for the K_t computations.

The calibration power level (in dBm) measured during the calibration sequence is converted to a voltage, as is the power measured at the spectrum analyzer for each measurement point. The phase is then computed as in the K_p measurement. Figure 9 shows a typical plot output for the AM-PM transfer coefficient measurement.

Earth station verification measurements

A new class of measurements, developed jointly by COMSAT Laboratories and EUTELSAT, uses the orbiting satellite as a calibrated signal source for performing independent ESVA measurements on a second earth station. The EUTELSAT IOT facility is located in one earth station—referred to as the earth reference station (ERS)—which performs the measurements. The second earth station is the station under test (SUT). Both stations must be able to access the satellite simultaneously. The operators at the stations coordinate their activities via telephone.

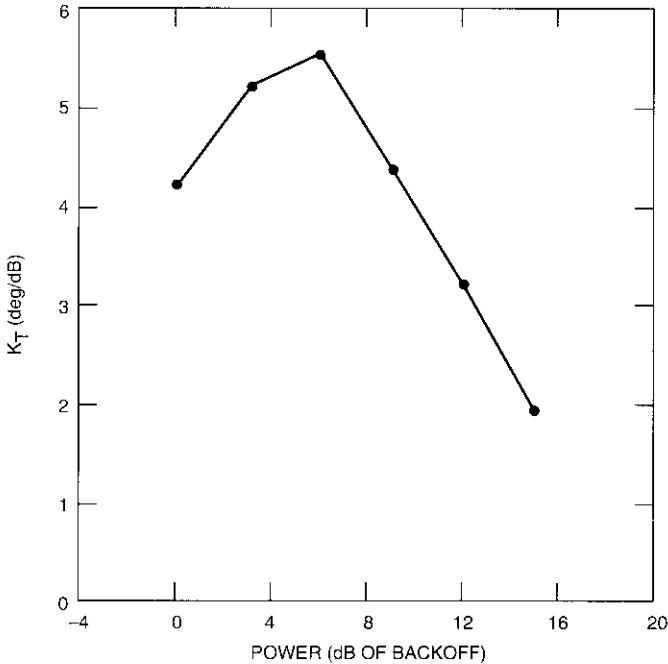


Figure 9. *AM-PM Transfer Coefficient Plot Output*

Four ESVA measurements have been developed and tested with an actual SUT: EIRP, G/T , transmit cross-polarization isolation, and SUT transmit antenna sidelobe pattern. References 4 and 5 contain additional information on ESVA measurement.

Because the ERS and SUT are generally off-axis relative to the spacecraft receive and transmit antennas, the spacecraft gain for the ERS and SUT signals is adjusted for the off-axis loss to the stations. The off-axis loss values are operator inputs to the measurements.

EARTH STATION EIRP MEASUREMENT

The objective of the earth station EIRP test is to verify the transmit capabilities of the SUT in terms of its accuracy and adjustment range. The basic principle of this test is that, since the ERS and SUT both transmit signals through the spacecraft at the same time and at nearly equal levels, the accuracy of the ERS measurement system will be transferred directly to the measurement of the SUT parameters. Figure 10 depicts the ESVA EIRP measurement configuration and the quantities involved.

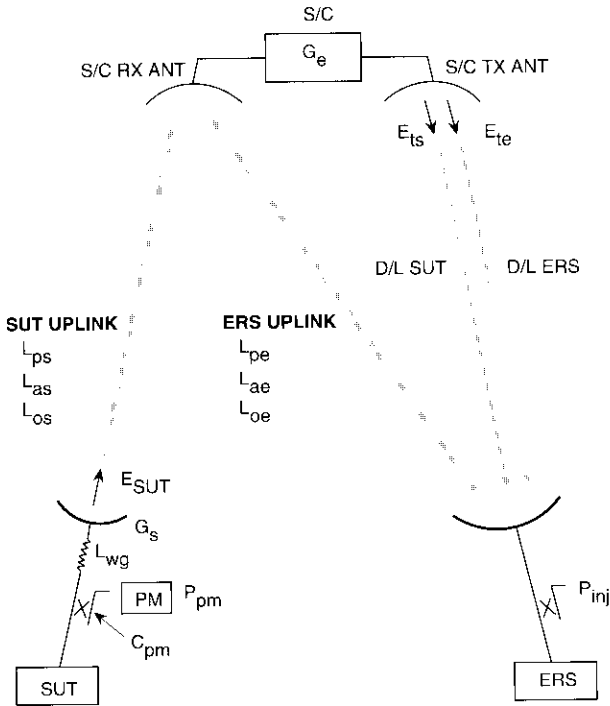


Figure 10. ESVA EIRP Measurement Configuration

The EIRP measurement is performed as follows. First, the operator is asked to ensure that the SUT is not transmitting. The operator then enters the following parameters via the measurement's user interface window:

- SUT uplink path loss (dB)
- SUT uplink atmospheric loss (dB)
- SUT transmit coupler calibration (dB)
- SUT transmit antenna waveguide loss (dB)
- SUT uplink off-axis loss (dB)
- ERS power range (dB)
- ERS power step (dB)
- ERS frequency offset from the SUT uplink (MHz)
- ERS EIRP (dBW)
- ERS uplink off-axis loss (dB)

- Maximum power balance delta between SUT and ERS (dB)
- Search bandwidth (MHz)

Next, the ERS uplink and downlink chains are configured for the measurement. The ERS transmits a signal and measures the local oscillator frequency of the spacecraft transponder being used. The ERS signal is then turned off, and the ERS operator is requested to instruct the SUT to begin transmitting. The frequency of the SUT downlink signal is measured by the ERS, which then transmits at a frequency that is offset from the SUT uplink frequency, at the power level specified by the operator. Both stations are now transmitting simultaneously to the spacecraft. The power level at which the ERS transmits takes into account the atmospheric attenuation at the ERS. The ERS and SUT uplink signals are "power-balanced" at the spacecraft's transmit antenna, as described below. The IOTE then measures the SUT station's transmit EIRP for each power level across the operator-specified range. Given the SUT antenna input power supplied to the ERS operator by the SUT operator, the SUT transmit antenna gain is calculated.

The ERS measures SUT power over a range of power levels specified by the operator input parameters. The input parameters are the power range (in dB), the power step size (in dB), and the initial level of the ERS transmit EIRP (in dBW) during the measurement setup phase. The measurement procedure is repeated for a typical 15-dB adjustment range of the SUT transmit EIRP level. The ERS EIRP power level (also an operator input) is used instead of the normal spacecraft saturation level as the backoff reference level.

For each power level in the sweep, the following steps are performed. The SUT operator is requested by the ERS operator to perform a power balance at the spacecraft's transmit antenna. When power balance is complete, the SUT operator provides the SUT uplink power meter reading to the ERS operator, who enters the value into the measurement. Power balance is achieved when the difference between the spacecraft's transmit EIRP due to the ERS uplink signal (E_{te} in Figure 10) and the spacecraft's transmit EIRP due to the SUT uplink signal (E_{ts} in Figure 10) is less than an operator-specified delta (typically 1 dB). The ERS then measures the spacecraft transmit EIRPs due to the SUT and ERS uplink signals. The ERS confirms the power balance at this point and computes the SUT earth station transmit EIRP.

The SUT's transmitted EIRP can be determined from the following quantities: the spacecraft transmit EIRP due to the SUT uplink signal, the spacecraft gain for the ERS uplink signal, the off-axis losses for the ERS and SUT, and the SUT's uplink path and atmospheric losses. The IOTE measures the spacecraft transmit EIRP due to the SUT signal. The SUT transmit EIRP is then calculated as follows:

$$E_{\text{SUT}} = E_{\text{ts}} - G_{\text{c}} + (L_{\text{os}} - L_{\text{oc}}) + L_{\text{ps}} + L_{\text{as}} \quad (5)$$

where

- E_{SUT} = SUT transmit EIRP (dBW)
- E_{ts} = spacecraft transmit EIRP due to the SUT uplink signal (dBW)
- G_{c} = spacecraft gain for the ERS uplink signal (dB)
- L_{os} = off-axis loss to the SUT (dB)
- L_{oc} = off-axis loss to the ERS (dB)
- L_{ps} = SUT uplink path loss (dB)
- L_{as} = SUT uplink atmospheric loss (dB).

Once the transmitted EIRP is determined, the antenna gain of the SUT can also be computed. With the SUT operator providing the waveguide loss of the SUT transmit antenna, the power meter reading of the SUT uplink carrier (in dBm), and the power meter coupler calibration, the antenna gain is computed according to

$$G_{\text{s}} = E_{\text{SUT}} + L_{\text{wg}} - P_{\text{pm}} - C_{\text{pm}} + 30 \quad (6)$$

where

- G_{s} = gain of the SUT transmit antenna (dB)
- L_{wg} = waveguide loss of the SUT transmit antenna (dB)
- P_{pm} = SUT uplink power meter reading (dBm)
- C_{pm} = SUT uplink power meter coupler calibration (dB).

The accuracy of this earth station antenna gain measurement at the ERS is comparable to that of the basic EUTELSAT IOTE EIRP measurement, with an expected small loss in accuracy due to dependence on the assumed values for the SUT parameters. Figure 11 shows a typical earth station EIRP plot output.

Earth station *G/T* measurement

The ESVA *G/T* test measures the *G/T* of the SUT, using the satellite as a calibrated signal source in the far field of the SUT antenna. Figure 12 depicts the *G/T* measurement configuration and the quantities involved.

The test derives the *G/T* of the SUT directly from two power measurements made with the SUT configured so that the output of the station down-converter is connected to an IF bandpass filter that has a calibrated noise bandwidth. The ERS sets its uplink power to the backoff level specified by the operator via the measurement's user interface. This backoff is referenced to the ERS maximum uplink EIRP specified by the operator (not to the spacecraft saturation level). The ERS transmits at this level.

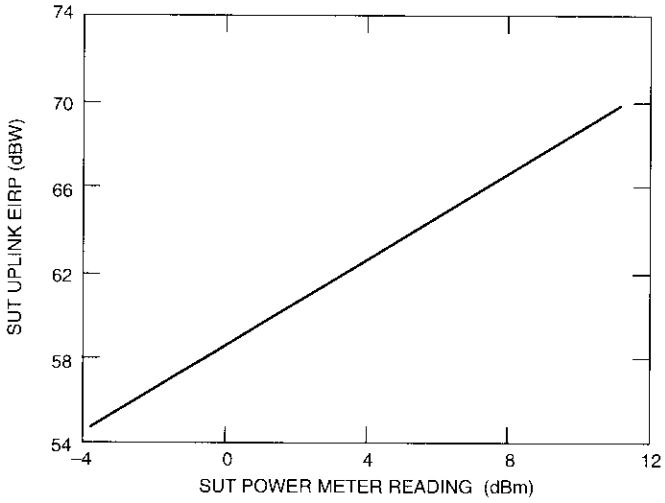


Figure 11. Earth Station EIRP Measurement Output

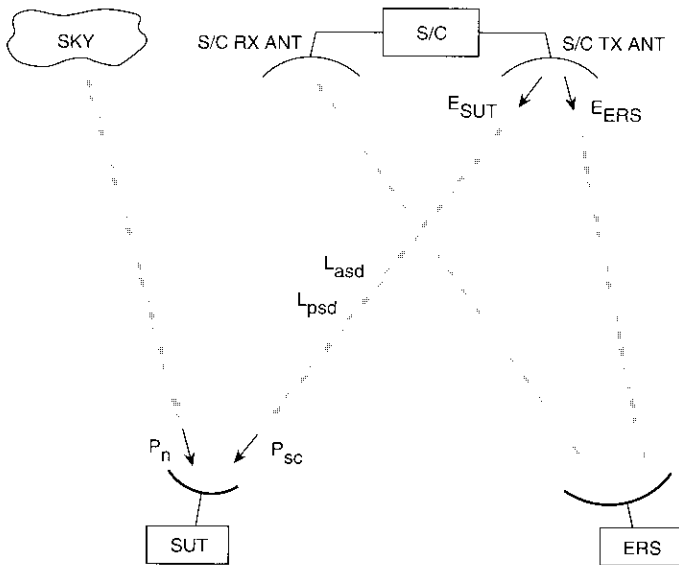


Figure 12. ESVA G/T Measurement

The SUT antenna is pointed toward the satellite, and the power, P_{sc} , at the filter output is measured. The SUT antenna is then pointed toward the sky, away from the satellite, and the noise power, P_n , at the filter output is measured. G/T is computed using P_{sc} and P_n .

The ERS uplink and downlink are configured for each channel being measured, and the local oscillator frequency of the spacecraft is measured, if it is different from that of the last channel. The uplink at the ERS is then set to the operator-specified backoff level from the specified maximum uplink power, and the IPFD and EIRP are measured. Next, the ERS operator enters the off-axis losses, as well as the downlink atmospheric and path losses, as seen from the SUT and provided by the SUT operator. The SUT operator is directed to measure the received power at the SUT, and then to move the SUT antenna away from the spacecraft and measure the noise received from the sky. The IOTE determines the spacecraft's transmit EIRP as seen at the SUT by calculating the spacecraft's transmit EIRP as seen at the ERS. The SUT G/T is computed as follows:

$$G/T_s = -228.6 + BW_s + L_{psd} + L_{asd} - E_{SUT} + 10 \times \log P_3 - CF \quad (7)$$

where

G/T_s = measured SUT G/T (dB/K)

-228.6 = dB equivalent of Boltzmann's constant

BW_s = SUT filter bandwidth (dB-Hz)

L_{psd} = SUT downlink path losses (dB)

L_{asd} = SUT downlink atmospheric loss (dB)

E_{SUT} = spacecraft EIRP seen by SUT (dBW)

$P_3 = (P_2/P_1 - 1)$

where

$$P_1 = 10^{(P_n/10)}$$

$$P_2 = 10^{(P_{sc}/10)}$$

CF = operator-entered correction factor (dB).

ESVA transmit polarization isolation measurement

This test measures the transmit polarization isolation of the SUT. In the EUTELSAT IOT, the test can be performed in both the X and the Y polarizations at various SUT antenna pointing angles. Figure 13 illustrates the ESVA transmit cross-polarization isolation measurement configuration and the quantities involved.

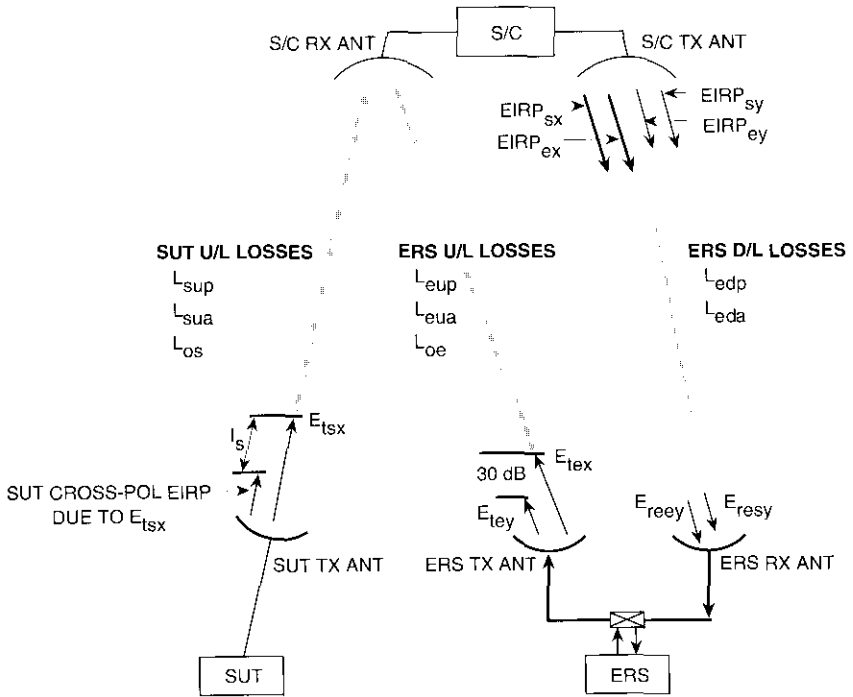


Figure 13. *ESVA Transmit Cross-Polarization Isolation Measurement*

When the SUT transmits a carrier in one polarization, a small amount of the carrier's power spills over, or leaks, into the opposite polarization transmit path due to imperfect isolation between the two paths. This leakage power is also transmitted in the opposite polarization. The SUT transmit cross-polarization isolation, I_s , between the two transmission paths measures the degree of isolation.

The measurement uses two spacecraft transponders: one designated as the copolarization (copol) transponder, and the other as the cross-polarization (cross-pol) transponder. First, the ERS operator configures the measurement by entering various parameters into the measurement's user interface window, and establishes communication with the SUT operator, who supplies SUT parameter values for entry via the user interface window. During the measurement, the ERS operator is prompted via dialog windows to provide input and perform various actions. The ERS operator is then requested to turn on the copol transponder and turn off the cross-pol transponder. The ERS configures

its uplink and downlink chains for the spacecraft channel being used and transmits an uplink carrier in the copol transponder at the center frequency of the channel. The downlink signal is received at the ERS, and the spacecraft's local oscillator frequency is measured. The SUT operator is then instructed to transmit at the same frequency and polarization as the ERS uplink carrier. The ERS stops transmitting, and the frequency of the SUT transmission is measured at the ERS. The ERS is returned to a frequency that is offset from the SUT uplink frequency, and then transmits at a backoff level relative to the maximum earth station uplink transmit EIRP allowed by the measurement program.

An interactive power balance procedure is now performed, as in the ESVA EIRP measurement. The balancing procedure ensures that the spacecraft transmit EIRP due to the ERS uplink carrier ($EIRP_{cc}$ in Figure 13) and the spacecraft transmit EIRP due to the SUT uplink carrier ($EIRP_{sx}$) differ by less than an operator-specified amount. The SUT copol transmit EIRP is designated as E_{tsx} , where the subscripts indicate transmission (t) by the SUT (s) in the arbitrarily chosen X polarization (x). Uplink and downlink parameters (path and atmospheric losses) are measured for both the ERS and SUT uplink and downlink carriers.

Next, the SUT operator is requested to turn off the SUT uplink carrier. The copol transponder is turned off, and the cross-pol transponder is turned on. The ERS then transmits a cross-pol carrier (*i.e.*, a carrier on the opposite polarization, E_{tey}) at the same frequency used in the copol measurement procedure above, but 30 dB down from the level transmitted by the ERS during the copol measurement (E_{tcx}) just performed.

At this time, a series of measurements are performed. The SUT operator is requested to transmit again in the copolarization at the level of E_{tsx} , as before. Some of the power from the SUT transmission of a copol uplink carrier leaks into the transmission path of the opposite polarization and is also transmitted by the SUT as a small cross-pol carrier. This undesirable carrier causes a corresponding spacecraft EIRP ($EIRP_{sy}$) to be transmitted. The ERS cross-pol uplink carrier, E_{tey} , causes a new level of spacecraft transmit EIRP, $EIRP_{ey}$. The uplink and downlink parameters for the ERS and SUT signals are measured for use in the cross-pol measurement.

The ERS operator is prompted for the SUT power meter reading, the SUT antenna azimuth or elevation, and the contour value of the SUT antenna gain. Based on the copol and cross-pol measurements just performed, the SUT antenna transmit isolation is computed (in dB) as follows:

$$I_s = E_{tsx} - (E_{resy} - E_{reey}) - E_{tey} - (L_{sup} - L_{cup}) - (L_{sua} - L_{cua}) + (L_{os} - L_{oe}) \quad (8)$$

where

- I_s = SUT transmit cross-pol isolation (dB)
- E_{tsx} = SUT transmit copol EIRP (dBW)
- E_{resy} = computed equivalent spacecraft EIRP at the ERS receive antenna due to the SUT transmit cross-pol carrier (dBW)
- E_{reey} = computed equivalent spacecraft EIRP at the ERS receive antenna due to the ERS transmit cross-pol carrier (dBW)
- E_{tcy} = earth station EIRP transmitted by the ERS in the cross-pol carrier (dBW)
- L_{sup} = SUT uplink path loss (dB)
- L_{eup} = ERS uplink path loss (dB)
- L_{sua} = SUT uplink atmospheric loss (dB)
- L_{eua} = ERS uplink atmospheric loss (dB)
- L_{os} = off-axis loss to the SUT (dB)
- L_{oc} = off-axis loss to the ERS (dB).

Because the SUT and ERS downlink frequencies are very close (typically 2 MHz apart at 12-GHz carrier frequencies), the measurement assumes that the difference in downlink losses for the ERS and SUT signals is negligible for the downlink path and atmospheric losses.

ESVA transmit sidelobe pattern measurement

This test, which measures the transmit sidelobe levels of the SUT transmit antenna, is performed to ensure that the SUT meets EUTELSAT specifications. Figure 14 depicts the ESVA transmit sidelobe measurement configuration and the quantities involved.

First, the SUT transmits in the linear region of the spacecraft TWTA gain transfer characteristic. It then slews the SUT antenna in azimuth or elevation, and the ERS measures the downlink power. Next, the SUT antenna is offset by 1° and the uplink power is increased by 15 dB. The SUT antenna is then steered away from beam center while the ERS measures the downlink power. This procedure is repeated for both sides of the SUT antenna beam. The ERS EIRP power level (an operator input) is used, instead of the spacecraft saturation level, as the backoff reference level. The measurements for each side of the SUT antenna beam are then combined in an interactive data analysis and manipulation software package and plotted to show the SUT antenna pattern.

A gain transfer measurement is performed, using the injected signal technique, and saved for later use in computing spacecraft transmit EIRP. The SUT

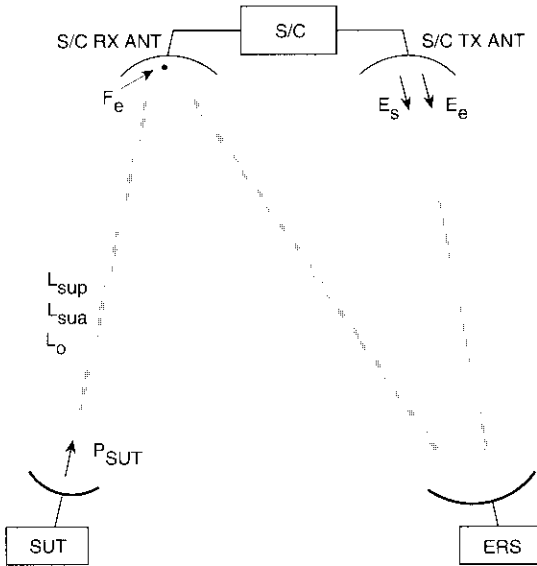


Figure 14. *ESVA Transmit Sidelobe Measurement*

is directed to turn off its transmitter during this measurement. The SUT then turns on its transmitter and transmits a carrier to the spacecraft, and the carrier's downlink frequency is measured by the ERS. The ERS transmits an uplink carrier at a frequency that is offset from the SUT uplink. The SUT and ERS signals are power-balanced, as in the ESVA EIRP measurement, and the ERS turns off its uplink signal.

The SUT is then directed to slew its antenna at a user-specified rate, and the measurement is initiated by the ERS operator via a dialog window and continues until stopped by the operator. For each SUT transmit EIRP measurement, the measurement program computes the antenna slew angle in real time, based on the initial angle, start time, and slew rate inputs supplied by the operator, and the time elapsed since the start.

The spacecraft EIRP due to the SUT uplink carrier is expressed in terms of the EIRP caused by the ERS uplink carrier and the levels measured on the spectrum analyzer for both downlink carriers, as follows:

$$E_s = E_e + (S_s - S_e) \quad (\text{dBW}) \quad (9)$$

where

$$E_s = \text{spacecraft transmit EIRP due to SUT carrier (dBW)}$$

E_c = spacecraft transmit EIRP due to ERS carrier (dBW)

S_s = received SUT signal measured on spectrum analyzer (dBm)

S_c = received ERS signal measured on spectrum analyzer (dBm).

The spacecraft transmit EIRP due to the SUT carrier can be obtained by measuring only three quantities: E_c , S_s , and S_c . The value for E_c and the associated signal level measured on the spectrum analyzer, S_c , are arbitrarily chosen as the first point in the gain transfer measurement performed earlier. The above relationship assumes the following:

- The ERS gain transfer measurement is performed using the injected signal technique.
- The ERS is not transmitting during measurement under slewing conditions.
- The SUT downlink carrier is at the same frequency and polarization as the gain transfer measurement.
- The injected signal power level is the same in both measurements.
- There is negligible change in the ERS distance to the spacecraft between the gain transfer measurement and the ERS EIRP measurement a few minutes later.
- Because the gain transfer and EIRP measurements are performed a few minutes apart, the downlink path loss, downlink atmospheric loss, ERS receive antenna gain, and inject signal coupler value are assumed to be constant during the measurement.
- The SUT antenna slews over the desired range in a few minutes. If the slew rate is a typical $0.02^\circ/\text{s}$, the SUT requires 5 minutes to slew 6° .

Since E_c and S_c were measured and stored during the gain transfer test, the spacecraft EIRP due to the SUT uplink carrier can be determined by measuring the received signal level on the spectrum analyzer while the SUT antenna is slewing in real time. The spectrum analyzer is set to a reference vertical scale level and left on that scale setting during the slew measurement. The measurement then makes successive and rapid readings of the voltage measured by the digital voltmeter and converts them to equivalent power in dBm. The above relationship [equation (9)] is used to compute the spacecraft transmit EIRP due to the SUT uplink carrier in real time and "on the fly," while the SUT antenna is slewing. Thus, it is not necessary to perform actual injected-signal EIRP measurements for the SUT signal. The relationship has been verified empirically with measurement data.

The spacecraft EIRP due to the SUT uplink carrier is converted to an equivalent spacecraft IPFD by linear interpolation from the gain transfer table stored previously. The gain transfer table gives the relationship of spacecraft IPFD to spacecraft transmit EIRP for the measured transponder. Since the data in the gain transfer table were measured with an uplink carrier from the ERS and not the SUT, the interpolated input flux for the SUT carrier must be corrected to compensate for the difference of the off-axis losses between the spacecraft and the respective earth stations.

The equivalent IPFD of the SUT carrier at the spacecraft receive antenna is converted to an equivalent EIRP, which can then be related to the SUT uplink EIRP. The SUT uplink and atmospheric losses are supplied by the SUT operator to the ERS operator, who enters these parameters into the measurement. The SUT transmit EIRP is then computed according to the following relationship:

$$P_{\text{SUT}} = F_e + L_o + 10 \log \frac{(c/f_s)^2}{4\pi} + L_{\text{sup}} + L_{\text{sua}} \quad (\text{dBW}) \quad (10)$$

where

P_{SUT} = SUT uplink EIRP (dBW)

F_e = input flux to the spacecraft that would have to be transmitted by the ERS to cause the same level of spacecraft transmit EIRP due to the SUT uplink signal (dBW/m²)

L_o = difference between the ERS off-axis loss and the SUT off-axis loss (dB)

c = velocity of light (m/s)

f_s = SUT uplink frequency (Hz)

L_{sup} = SUT uplink path loss (dB)

L_{sua} = SUT uplink atmospheric loss (dB).

The SUT uplink antenna gain is determined relative to the measurement starting point gain by computing the delta between the reference starting point SUT uplink EIRP value and the measured uplink EIRP, and subtracting the deltas from the reference gain level.

For each SUT uplink EIRP measurement, the IOTE computes the slew angle based on the initial angle, start time, slew rate, and elapsed time. The initial SUT angle, the SUT antenna slew rate, and the SUT starting slew time are supplied by the SUT operator to the ERS operator, who inputs them into the measurement. Finally, the procedure measures the elapsed time since the start of the measurement. Figure 15 shows typical data for a single-sided earth station transmit sidelobe measurement.

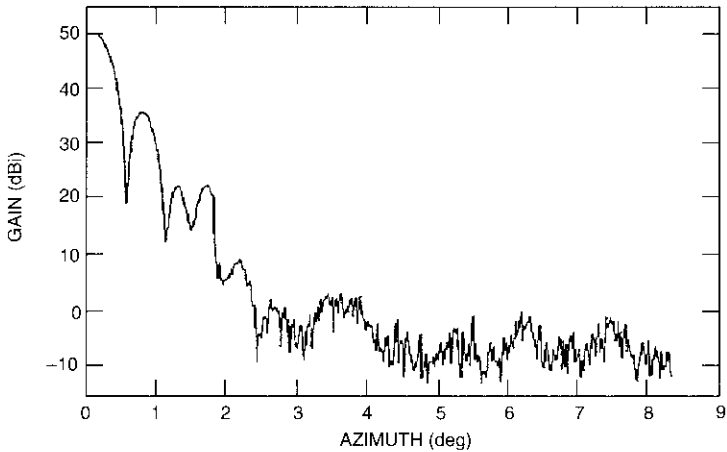


Figure 15. *Earth Station Transmit Sidelobe Measurement*

Conclusions

The continuing trend toward higher-capacity, more complex communications satellites, such as the EUTELSAT II series, places greater demands and constraints on the IOT systems built to test them. Because of the larger number of transponders and configurations to be tested and the expanded repertoire of tests to be performed, a modern IOT system must acquire and analyze an increasing volume of test data. This situation tends to lengthen the testing time required, which conflicts with the owner's desire that the satellite be placed into operational, revenue-generating service as soon as possible after launch.

A UNIX workstation-based, highly automated IOT system installed at the EUTELSAT earth station in Rambouillet, France, includes several innovative features and measurements. The X-Window-based graphical user interface provides operational flexibility and is easier to use than older, command-line interfaces. The system's scheduler permits unattended stability measurements to be performed at specified intervals by sharing equipment and earth station resources among IOT measurements. A new technique called Fast sweep reduces the time needed to measure a spacecraft channel's frequency response from several minutes to a few seconds, using an asynchronous swept-frequency measurement technique and post-measurement digital processing. The use of the spacecraft as a calibrated far-field signal source enables EUTELSAT to independently measure and evaluate the performance characteristics of a second earth station.

The EUTELSAT IOT system was developed to support EUTELSAT's testing of its second-generation satellites, and has been used for the IOT of the EUTELSAT II F1, F2, F3, and F4 spacecraft.

Acknowledgments

The authors would like to acknowledge the following individuals. C. Mahle of COMSAT Laboratories has been a constant source of help and encouragement. His past and current contributions to this work are major. S. Bangara, currently with INTELSAT, played a key role in defining the system requirements for the EUTELSAT IOTE, and R. Issler of DTRE made significant contributions to the IOTE-ECCS interface implementation and testing. The DTRE staff at the Rambouillet earth station are acknowledged for their assistance and support during the system installation, testing, and deployment of the EUTELSAT IOTE.

The earth station (excluding the IOTE/MMS) was made available to EUTELSAT by DTRE, the overseas arm of the French Post, Telephone, and Telegraph Administration (PTT). The ECCS computer and its station control and status software are supplied to EUTELSAT by DTRE.

References

- [1] I. Dostis *et al.*, "In-Orbit Testing of Communications Satellites," *COMSAT Technical Review*, Vol. 7, No. 1, Spring 1977, pp. 197-226.
- [2] A. F. Standing, *Measurement Techniques for In-Orbit Testing of Satellites*. Computer Science Press, New York: W. H. Freeman, 1990.
- [3] C. E. Mahle, "In-Orbit Testing of Commercial Communications Satellites," 23rd General Assembly of the International Union of Radio Science (URSI), Prague, Czechoslovakia, August-September 1990.
- [4] Y. Tharaud, B. Kasstan, and P. Barthmann, "IOT System for the EUTELSAT II Satellites," IEEE Global Satellite Communications Symposium, Nanjing, China, May 1991, *Proc.*, pp. 168-177.
- [5] Y. Tharaud and V. Riginos, "EUTELSAT's Facilities for Measurement of Earth Stations and In-Orbit Satellite Payloads," 23rd General Assembly of the International Union of Radio Science (URSI), Prague, Czechoslovakia, August-September 1990.
- [6] V. Riginos, P. Shen, and S. Bangara, "In-Orbit Testing of Communications Satellites: The State of the Art," IEEE Global Satellite Communications Symposium, Nanjing, China, May 1991, *Proc.*, pp. 150-159.
- [7] S. K. Card, T. P. Moran, and A. Newell, *The Psychology of Human-Computer Interaction*, Hillsdale, NJ: Lawrence Erlbaum, 1983.

- [8] K. D. Fullett *et al.*, "Microwave Measurement Software System," *COMSAT Technical Review*, Vol. 23, No. 1, Spring 1993, pp. 101-137 (this issue).
- [9] K. D. Fullett and V. E. Riginos, "Error Analysis of In-Orbit Measurements on Communications Satellites," 23rd General Assembly of the International Union of Radio Science (URSI), Prague, Czechoslovakia, August-September 1990.
- [10] Hewlett-Packard, "Phase Noise Characterization of Microwave Oscillators," HP Product Note No. 11729B-1.



Kenneth D. Fullett received a BSEE and MSEE from the University of Illinois, Urbana-Champaign, in 1979 and 1981, respectively. He joined COMSAT Laboratories in 1981 as a member of the Transponders Department of the Microwave Technology Division and participated in all aspects (including both microwave hardware and computer software system design) of many IOT systems, including those for INTELSAT, MCI, and EUTELSAT. His work also involved software development for COMPACT Software, and he was a project manager for the RF Terminal Supervisory System of the NASA/ACTS earth station. Mr. Fullett

is currently engaged in high-energy physics research in the Anti-Proton Source Department of the Accelerator Division of Fermi National Accelerator Laboratory, Batavia, Illinois.

Bernard J. Kasstan received an Honours degree in physics and electronics from Newcastle-upon-Tyne Polytechnic, U. K., in 1981; and a Masters degree in telecommunications from the University of Essex in 1982. He subsequently conducted research on tropospheric propagation on earth-to-satellite paths. He joined EUTELSAT in 1984, and was responsible for the verification of new earth stations in the EUTELSAT space segment. In 1987, he moved to IOT activities, including payload subsystem performance evaluation, investigations of payload anomalies in orbit, and supervision of IOT installation at the host stations. In

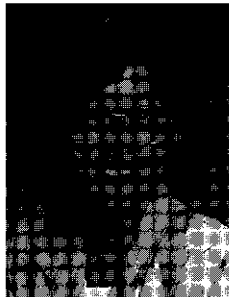
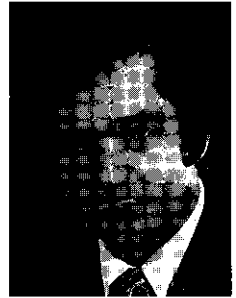


conjunction with the System Verification Test Section, Mr. Kasstan has developed new IOT techniques that have been discussed in numerous published papers.



Walter D. Kelley, Jr., earned a BS in electrical engineering at the Catholic University of America, Washington, D.C., in 1974; and an MBA at Marymount University, Arlington, VA, in 1983. In 1991, he joined the Transponders Department of the Satellite and Systems Technologies Division at COMSAT Laboratories as a Member of the Technical Staff. At COMSAT, he has participated in development of the IOT system for Hughes Communications' DirecTv™, an IOT system for EUTELSAT, and the NASA/ACTS ground station control and status subsystem.

Vasilis E. Riginos received a BE, MEng, and PhD in electrophysics from the Stevens Institute of Technology, Hoboken, NJ, in 1964, 1970, and 1973, respectively. He is currently Manager of the Transponders Department of the Satellite and Systems Technologies Division at COMSAT Laboratories, where he is responsible for directing research and development on communications system performance as applied to satellite transponders. He also supervises research and development in advanced microwave circuits such as high-power amplifiers, regenerative receivers, filters, and multiplexers. Dr. Riginos participated in the evaluation of the Inmarsat program, and has been project manager for the GTE ATEF IOT system, the INTELSAT Maritime Communications Subsystem IOI station, the EUTELSAT IOT system, and the Hughes DirecTv™ IOT system. He is a member of Sigma Xi, AAAS, IEEE, and the American Physical Society.



Pei-Hong Shen received a BS and MS in genetics, and an MS in computer science, from Washington State University in 1983, 1984, and 1986, respectively. From 1978 to 1981, she studied biology and genetics while attending Fudan University in Shanghai, Peoples Republic of China. Ms. Shen is currently a Senior Member of the Technical Staff in the Transponders Department of the Satellite and Systems Technologies Division at COMSAT Laboratories, where she is primarily responsible for design and development of software for communications satellite applications. Since joining COMSAT in 1987, she has been involved in the design and development of the following systems: NASA/ACTS, EUTELSAT IOT, and Hughes' DirecTv™ IOT. She is a member of the IEEE Computer Society.



Steven L. Teller received an AS and AA from Harper College in 1979; and a BA in information and computer sciences from Hood College in 1991. He is currently a Member of the Technical Staff in the Transponders Department of the Satellite and Systems Technologies Division at COMSAT Laboratories. Since joining COMSAT, he has been involved in various aspects of the IOT of communications satellites, including the NASA/ACTS RF terminal supervisor, and IOT for EUTELSAT, MCI, INTELSAT, GTE, and the Hughes DirecTV™ system. He

has been responsible for software vs manual measurement verification during system development, in-plant testing, and on-site testing. He was also involved in prototyping and testing various new measurement schemes, and was a major contributor to final system installation testing.

Yves Tharaud received an MSc in electronics, electrotechnology, and automatics from the University of Bordeaux, France, in 1974; and the title of Engineer from the Ecole Nationale Supérieure d'Electronique et de Radioélectrique de Bordeaux in 1975. He joined EUTELSAT in 1981 and participated in the definition and implementation of new facilities dedicated to IOT, earth station verification and assistance (ESVA), and payload traffic monitoring for the EUTELSAT II satellites. He served as manager of the System Verification Test Section in the Operations Department, where he supervised activities related to satellite payload IOT and ESVA. Mr. Tharaud cooperated with the European Space Agency in similar activities on the ECS satellites and participated in the payload IOT and various other experiments on the OTS satellite as a member of the CNET in FRANCE TELECOM.

